

1967

# Negative resistance in cadmium sulfide.

John William Mohr



Department:

# NEGATIVE RESISTANCE

# IN

# CADMIUM SULFIDE

BY

JOHN W. MOHR

---

A

THESIS

Submitted to the Faculty of the

UNIVERSITY OF MISSOURI AT ROLLA

in Partial Fulfillment of the Requirements for the

Degree of

MASTER OF SCIENCE IN ELECTRICAL ENGINEERING

Rolla, Missouri

1967



---

Approved by

Norman Dillman (Advisor)

Charles A. Gobar

Albert E. Poston

R. D. Chenoweth

# ABSTRACT

A light-sensitive, negative-resistance phenomenon has been observed in a special two-terminal CdS device fabricated from selected single crystals. The device differs from those used in previous investigations in that one end of the device was masked to keep out visible light and that the phenomenon was observed at room temperature. A method is described which enables the phenomenon to be observed on a reproducible basis. It was found that the CdS single crystal must have a relatively high density of traps. Possible mechanisms which may contribute to the phenomenon are discussed.

# ACKNOWLEDGMENTS

The author wishes to express his appreciation to Dr. N. G. Dillman for his assistance and guidance throughout the investigation, to Earl Worstell and Art Reckinger for their many helpful discussions with the author, and to the Electronics Division of Eagle-Picher Industries for supplying the CdS single crystals used in this investigation. This investigation was funded by the Space Sciences Research Center of the University of Missouri.

TABLE OF CONTENTS

ABSTRACT . . . . . ii

ACKNOWLEDGEMENTS . . . . . iii

LIST OF FIGURES . . . . . v

LIST OF TABLES . . . . . vi

I. INTRODUCTION . . . . . 1

II. REVIEW OF LITERATURE . . . . . 5

III. FABRICATION OF THE DEVICE . . . . . 11

A. Preparation of the CdS bar . . . . . 11
B. Contacts . . . . . 13
C. Mask . . . . . 13

IV. EXPERIMENTAL METHODS . . . . . 16

A. Optical Measurements . . . . . 16
B. Electrical Measurements . . . . . 17

V. EXPERIMENTAL RESULTS . . . . . 20

A. General Results . . . . . 20
B. Device 16 Results . . . . . 23
C. Conclusions . . . . . 30

VI. POSSIBLE MECHANISMS . . . . . 39

VII. SUMMARY AND RECOMMENDATIONS . . . . . 41

A. Summary . . . . . 41
B. Recommendations for Further Studies . . . . . 41

BIBLIOGRAPHY . . . . . 43

VITA . . . . . 45

# LIST OF FIGURES


| Figure | | Page |
|---|---|---|
| 1 | Current-Voltage Curve for Special Two-Terminal CdS Single Crystal Device. . . . . | 2 |
| 2 | Special Two-Terminal CdS Device . . . . . | 12 |
| 3 | Block Diagram of Equipment Set-Up . . . . . | 18 |
| 4 | Output Waveform of Function Generator . . . . . | 19 |
| 5 | Current-Voltage Curves for Device 16 Operating in the A and D Configurations. . . . . | 22 |
| 6 | Current-Voltage Curve for Device 16 Operating in the A Configuration . . . . . | 24 |
| 7 | Current-Voltage Curve for Device 16 Operating in the B Configuration . . . . . | 26 |
| 8 | Current-Voltage Curve for Device 16 Operating in the C Configuration . . . . . | 27 |
| 9 | Current-Voltage Curve for Device 16 Operating in the D Configuration . . . . . | 28 |
| 10 | Log Current-Log Voltage Curve for Device 16 Operating in the A Configuration . . . . . | 29 |
| 11 | Current-Voltage Curve for Device 16 Operating in the E Configuration . . . . . | 31 |
| 12 | Current-Voltage Curve for Device 16 Operating in the F Configuration . . . . . | 32 |
| 13 | Current-Voltage Curve for Device 16 Operating in the G Configuration . . . . . | 33 |
| 14 | Current-Voltage Curve for Device 16 Operating in the H Configuration . . . . . | 34 |
| 15 | Log Current-Log Voltage Curve for Device 16 Operating in the E Configuration . . . . . | 35 |
| 16 | Current-Voltage Curves for Device 16 Operating in the A Configuration at Two Different Light Intensities. . . . . | 36 |

# LIST OF TABLES


| Table | | Page |
|---|---|---|
| I | General Data on Cadmium Sulfide . . . . . | 3 |
| II | Physical Properties of Cadmium Sulfide. . . . . | 3 |
| III | Devices Fabricated. . . . . | 14 |
| IV | Contact Fabrications. . . . . | 15 |
| V | Device Configurations . . . . . | 21 |
| VI | Properties of CdS Single Crystal 1-S331 . . . . . | 37 |

# I. INTRODUCTION

The scope of the work described in this document is the investigation of negative resistance in a special two-terminal cadmium sulfide (CdS) single-crystal device. Figure 1 illustrates a typical current-voltage characteristic curve for the device at room temperature. CdS was used because it is very photosensitive and large single crystals are available. Tables I and II contain general data on CdS, and the physical properties of CdS, respectively.

The device was originally conceived by Dillman[1]. It consists of a bar of single-crystal CdS approximately 2 mm by 2 mm in cross section with a length of approximately 10 mm. A rectifying contact of silver (Ag) is attached to one end of the bar and an ohmic contact of indium (In) is on the opposite end. One half of the device, including the Ag contact, is masked to keep out visible light. The other half is exposed to visible light.

This document is divided into six additional parts as follows: (1) Section II is a review of literature citing previous work done in the field of negative resistance in CdS, (2) Section III describes the fabrication of the device used in the investigation, (3) Section IV describes the methods used to observe the negative-resistance phenomenon in the DC current-voltage characteristics of the device at room temperature, (4) Section V contains the results of the investigation, which are used to determine the conditions

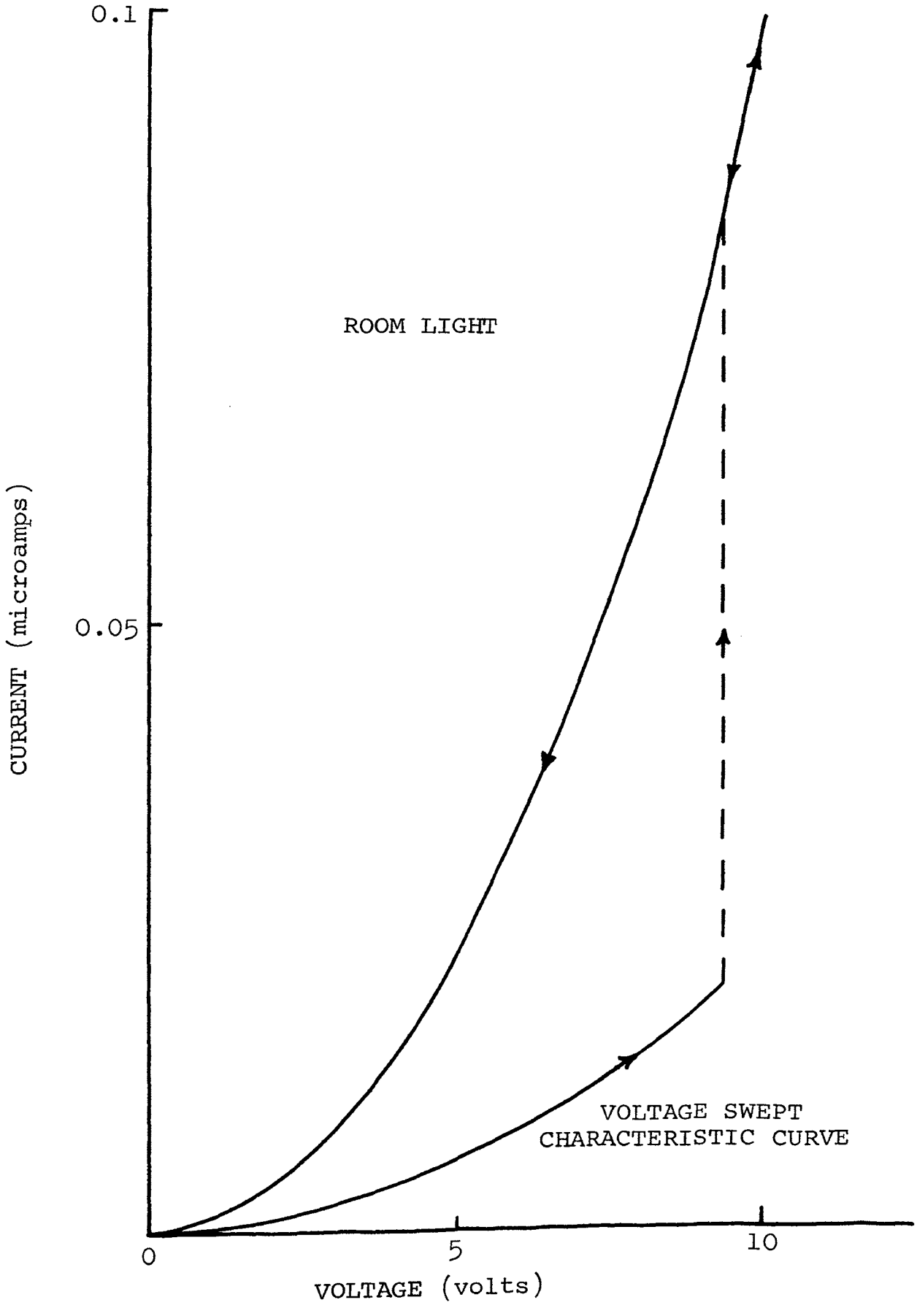


Figure 1. Current-Voltage Curve for Special Two-Terminal CdS Single Crystal Device.

Table I. General Data on Cadmium Sulfide

| | |
|---|---|
| Classification | II-VI Semiconductor |
| Type | N |
| Crystal Structure | Hexagonal |
| Band Gap Energy | 2.42 eV |
| Gap Transition | Direct |
| Absorption Edge | 500 mμ |
| Electron Mobility (Pure Crystal at 300°K) | 340 $cm^2$/(volt)(sec) |
| Dielectric Constant (Dark) | 10.3 |
| Lattice Constant a | 4.137 A° |
| Electron Affinity | 4.5 eV |
| Typical Dopants | Cl, Br, I, Al, Ga, In |
| Chief Use | Photoconductor |

Table II. Physical Properties of Cadmium Sulfide

| | |
|---|---|
| Specific Weight | 4.82 |
| Soluble | $HNO_3$ |
| Melting Point | 1500°C±15° at 50 atmosphere of Argon |
| Knoop Hardness | 122±4 with 25 gram load using Bergsman attachment to Vickers Microscope |
| Thermal Conductivity (300°K) | 0.024 cal/(sec)($cm^2$)(°K/cm) |
| Thermal Expansion (300-350°K range) | $4.2 \times 10^{-6}$/°C |

under which the negative-resistance phenomenon can be made to be reproducible, (5) Section VI is a discussion of possible mechanisms which may cause the negative-resistance phenomenon and (6) Section VII contains a summary of the investigation and some suggestions for further studies of the device.

## II. REVIEW OF LITERATURE

Negative resistance was predicted in a double-injection semi-insulator theory by Lampert[2]. Double injection in insulators was analyzed by taking into account the fact that the life-times for the injected electrons and holes are different and vary with injection level. The negative resistance has its origin in an increasing hole lifetime with increasing injection level, owing to electron depopulation of the recombination centers by hole capture. Assuming charge neutrality, a detailed solution was obtained for the simple model of an insulator with a single set of recombination centers filled with electrons in thermal equilibrium. He comments that the negative resistance should produce either current oscillations or a hysteresis in the DC current-voltage characteristics.

Smith[3] reported a hysteresis in the DC current-voltage characteristics of certain insulating CdS crystals with Ga contacts. The hysteresis was interpreted as the onset of double injection. He asserts that double injection is inferred from the observation of field-induced recombination radiation. The field in the bulk of the crystal was on the order of 1000 V/cm. Ambient temperatures were $77^{\circ}K$, $197^{\circ}K$, $300^{\circ}K$, and $353^{\circ}K$.

Light-sensitive, negative-resistance characteristics, arising from double-carrier injection in a trap-filled semi-insulator, have been observed in selected CdS single-crystals by Litton and Reynolds[4]. The double injection,

occurring at the Ag and In contacts, was accompanied by relatively intense light emission in the neighborhood of the Ag contact at field strengths often less than 10 V/cm. The potential of the Ag contact was positive with respect to the In contact. After appropriate light stimulation of the crystals, reproducible negative resistance was observed at $4.2^{\circ}K$ and nonreproducible negative resistance was observed at $77^{\circ}K$. The negative resistance did not occur at $77^{\circ}K$ in the same crystal that exhibited negative resistance at $4.2^{\circ}K$, even when it was stimulated to the same resistance and the same voltage was applied. Contact breakdown was ruled out as the double-injection mechanism because, under the conditions of contact breakdown, such breakdown would occur at both temperatures.

Dillman[1] observed nonreproducible negative resistance at room temperature in the DC current-voltage characteristics of a special two-terminal CdS device. One end of the single crystal bar, including the Ag contact was masked to keep out visible light. The potential of the Ag contact was negative with respect to the In contact. The average field strengths were less than 10 V/cm. The longitudinal axis of the bar was parallel to the c-axis of the crystal. The principles of the negative-resistance phenomenon were not examined.

The conditions for the presence of thermally-induced negative resistance were examined experimentally for CdS

and CdSe by Hansch, Nebauer, and Nikolaus[5]. The theoretically predicted change in the characteristics was observed by means of variations in the ambient temperature. A method is given which allows one to estimate the influence of Joule heating in investigations of other effects which lead to negative resistance.

Takagi and Mizushima[6] have observed negative resistance in the DC current-voltage characteristics of single-crystal films of CdS in the dark at room temperature. Fields were on the order of $1.5 \times 10^5$ V/cm. The c-axis of the crystal was in the plane surface of the film. The characteristics changed little at liquid nitrogen temperature. That fact, together with symmetry of polarity, made it difficult to explain the phenomenon on the basis of double injection. They comment that the mechanism may possibly be avalanche injection.

Ridley[7] discussed the two cases of negative resistance (voltage-controlled and current-controlled) which result from true bulk properties rather than from junction or contact phenomena. In the case of voltage-controlled negative resistance, it was shown that domains of high electric field occur. In the case of current-controlled negative resistance, it was shown that high current filaments form.

Current oscillations in CdS have been observed by Guerci, Melchiorri, and Melchiorri[8]. The oscillations varied with light intensity. The effect was attributed to

the diffused In contacts to the single crystal. It was argued that the contacts became non-ohmic in the applied electric field causing the current to vary.

McLeod and Hayes[9] observed current oscillations at room temperature in a single-crystal CdS bar only when the positive end of the bar was shaded. Ohmic contacts were formed on both ends of the bar by melting In onto the contact surfaces. The longitudinal axis of the bar was perpendicular to the c-axis of the crystal. The required dark portion of the positive end of the bar seemed to remain fixed at approximately 1 mm for various bar lengths used. Field strengths varied from 900 V/cm to 2700 V/cm depending on the bar length. Over a period of weeks the resistance of the contacts and crystals would increase as much as 5 to 1 with an accompanying increase in the start-oscillation voltage. The phenomenon was said to be difficult to explain on the basis of an acoustic resonant cavity model.

Yee[10] observed current oscillations in a dark conductive CdS bar when the electron drift velocity exceeded the velocity of sound waves. The fields were 820 V/cm and 1200 V/cm at $77^{\circ}K$ and $300^{\circ}K$, respectively. The longitudinal axis of the bar was parallel to the c-axis of the crystal. The oscillations were not sensitive to surface treatments, indicating that the phenomenon was either a bulk or contact effect. The mechanism was described as the propagation of high-field domains by the interaction of sound waves and free conduction carriers.

The room temperature conductivity of photosensitive crystals of CdS, rested long in the dark has been shown by Harnik[11] to be many orders of magnitude higher than its thermal equilbrium value, as a result of an effective isolation from the conduction band of holes trapped in the sensitizing centers during previous photoexcitation. The thermal or photo release to the valence band of these holes gives rise to a quenching of the conductivity.

Smith[12] made probe examinations of the potential distribution in single crystals of CdS. The measurements were taken at room temperature and represent static characteristics. The results of these measurements can be summarized as follows: (1) a uniform, linear potential distribution along the length of a crystal is the exception, rather than the rule, (2) generally the largest fraction (over 90 per cent) of the total potential drop is concentrated at either one or both ends of the crystal, (3) the potential drop at the ends is usually independent of the applied polarity, (4) the potential drop between any two points on the crystal is usually a very complicated function of light intensity, (5) a few CdS crystals have been found with an essentially linear potential distribution along their length and (6) relatively large (10 microamps to 1 milliamp) photocurrents have been drawn through crystals with linear potential distributions. He comments that the origin of the barriers at the electrodes is not well understood, and efforts to alter them artificially, or produce crystal-

electrode systems without barriers, generally have met with little success. He warns that before making calculations involving the electric field, it is advisable to actually measure the potential distribution rather than to assume it to be uniform.

Bube[13] has shown that when a photoconductor receives nonuniform illumination, some special effects can be obtained. He gave a brief example of a photoconductor illuminated parallel to the applied field by light which is strongly absorbed and produces excitation only to a certain depth. Either primary or secondary photoconductivity could result from the nonuniform illumination, depending on the relationship between the dielectric relaxation time and the transit time. Stockman[14] has discussed the problem of nonuniformly illuminated photoconductors without considering trapping. Rose[15] included the effects of trapping in his discussion of nonuniformly illuminated photoconductors.

Van Heerden[16] set up a criterion for the type of photocurrent (primary or secondary) to be expected from nonuniform illumination of a photoconductor. He supplemented observations on CdS by other authors to demonstrate that a primary photocurrent could be observed in insulating crystals. No correlation was found between the primary photocurrent and the presence of edge luminescence in the crystals.

# III. FABRICATION OF THE DEVICE

Figure 2 is an illustration of the special two-terminal CdS device described in Section I. Eighteen of the devices were fabricated from a selection of seven different CdS single crystals. The number of devices fabricated from a certain crystal was limited by the size and shape of the crystal. The differences, which were introduced during the fabrication of the devices are described as they are applicable. Table III lists these devices and their relative differences.

## A. Preparation of the CdS Bar

All of the CdS single crystals used in this investigation were grown by the vapor phase technique at the Electronics Division of Eagle-Picher Industries. After the c-axis of the CdS single crystal was determined by optical orientation, a flat slab approximately 3 mm thick was cut from it with a diamond saw. The slab was then hand ground on a wet surface grinder until it was approximately 2 mm thick. A bar approximately 2 mm wide by approximately 10 mm long was cleaved from the slab. Most of the bars were cleaved so that their longitudinal axis was parallel to the c-axis of the crystal. The others were cleaved so that their longitudinal axis was perpendicular to the c-axis of the crystal.

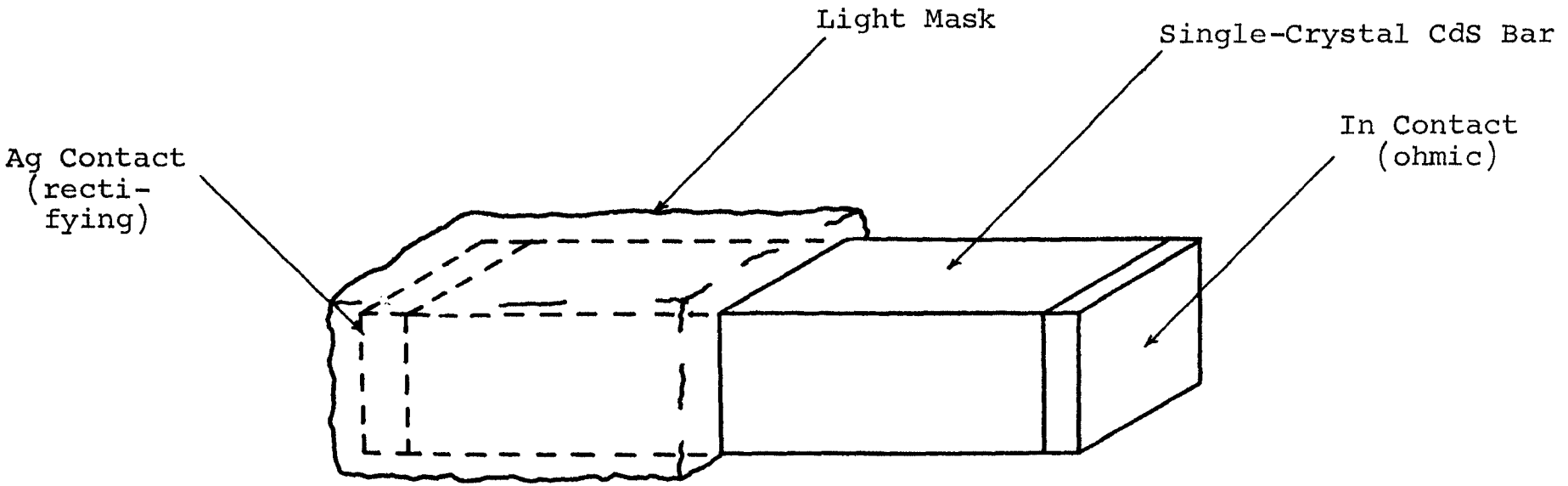


This drawing is approximately ten times the actual size of the device.

Figure 2. Special Two-Terminal CdS Device

B. Contacts

Every device fabricated used In for the ohmic contact and Ag for the rectifying contact. The method by which the contact was applied and the contact surface to which it was applied, varied with devices. Prior to applying any type contact, the contact surface was cleaned with ethanol. Table IV lists the different contact fabrications which were fabricated as follows: (1) Ag print brushed on a cleaved surface and air dried, (2) Ag print brushed on an acid (HCl) etched surface and air dried, (3) Ag print brushed on an abraded surface and air dried, (4) In soldered to a cleaved surface, (5) In soldered to an acid etched surface, (6) In soldered to an abraded surface, (7) cleaved surface dipped in molten In, (8) acid etched surface dipped in molten In, (9) abraded surface dipped in molten In and (10) vacuum deposited In on an abraded surface.

C. Mask

The light mask used to cover the half of the device including the Ag contact was a small piece of black vacuum sealing compound which was formed over the device. It also served the purpose of holding the device in place in the sample holder. The mask is a good electrical insulator.

Table III. Devices Fabricated

| DEVICE NUMBER (NOTE 1) | CRYSTAL NUMBER (NOTE 2) | AXIS (NOTE 3) | RECTIFYING CONTACT FABRICATION (NOTE 4) | OHMIC CONTACT FABRICATION (NOTE 4) |
|---|---|---|---|---|
| 1 | 1-116 | Parallel | (1) | (7) |
| 2* | 1-116 | Perpendicular | (1) | (7) |
| 3* | 001-24-8 | Parallel | (2) | (8) |
| 5* | 315 | Perpendicular | (1) | (7) |
| 6* | 3-120 | Parallel | (3) | (6) |
| 7 | 909-19-8 | Parallel | (2) | (5) |
| 9* | 3-118 | Parallel | (3) | (6) |
| 11 | 315 | Parallel | (1) | (7) |
| 12 | 1-S331 | Perpendicular | (3) | (9) |
| 13 | 1-S331 | Parallel | (2) | (5) |
| 14* | 1-S331 | Parallel | (1) | (4) |
| 16 | 1-S331 | Parallel | (3) | (10) |
| 17 | 1-S331 | Parallel | (3) | (6) |
| 18 | 1-S331 | Parallel | (3) | (9) |

NOTES: (1) Missing numbers indicate that a device was damaged before data could be taken. * indicates a device damaged after data was taken.

(2) Eagle-Picher lot number

(3) Long-axis of bar with respect to c-axis of crystal

(4) Refer to Table IV

Table IV. Contact Fabrications

| FABRICATION NUMBER | CONTACT TYPE | CONTACT METAL | CONTACT SURFACE (CdS) PREPARATION | CONTACT APPLICATION METHOD |
|---|---|---|---|---|
| (1) | Rectifying | Ag | Cleaved | Ag Print |
| (2) | Rectifying | Ag | Acid Etched | Ag Print |
| (3) | Rectifying | Ag | Abraded | Ag Print |
| (4) | Ohmic | In | Cleaved | Soldered |
| (5) | Ohmic | In | Acid Etched | Soldered |
| (6) | Ohmic | In | Abraded | Soldered |
| (7) | Ohmic | In | Cleaved | Dipped |
| (8) | Ohmic | In | Acid Etched | Dipped |
| (9) | Ohmic | In | Abraded | Dipped |
| (10) | Ohmic | In | Abraded | Vacuum Deposited |

# IV. EXPERIMENTAL METHODS

A device holder was constructed and used in making all the measurements during the investigation. It consisted of a light-tight box with all inside surfaces coated with optical flat black paint. The cover of the device holder could be opened or closed. The device rested in the device holder on a flat slab of plexiglass which was also painted flat black. Plexiglass was used because it is a good electrical insulator. Contact was made to each end of the device by slight pressure from a gold-tipped phosphor-bronze wire. The light mask held the device on the plexiglass slab in the proper position between the contacting wires.

All measurements were made at room temperature. Device temperatures were not monitored during the current-voltage measurements, and it is assumed that there was no appreciable temperature change as a consequence of ohmic heating.

## A. Optical Measurements

The relative intensity of the light incident on the device was measured with an Optics Technology Model 610 Power Meter. The instrument was designed to measure and give direct readings of the incident power from a laser beam in milliwatts. For the investigation it served the purpose of making relative light intensity measurements with readings in arbitrary units.

Illumination was provided by either the ambient room light or by a tungsten lamp. Dark measurements were made by closing the cover of the device holder.

All of the devices were very sensitive to variations in illumination, and for that reason, it was necessary for all objects in the room in which the measurements were being taken, to remain motionless during the measurement.

B. Electrical Measurements

Figure 3 is a block diagram of the equipment set-up used to obtain the DC current-voltage characteristic curves of the device directly without the need to take point by point data.

Figure 4 is an illustration of the output waveform of the Hewlett-Packard Model 202A Low Frequency Function Generator, which was used to provide a voltage sweep for the measurement system.

The analog output (calibrated) of the Hewlett-Packard Model 412A DC Vacuum Tube Voltmeter was used to drive the X channel of the Hewlett-Packard Model 7000A X-Y Recorder. The input impedance of the Model 412A voltmeter was 200 MΩ on all ranges used.

The analog output (calibrated) of the Hewlett-Packard Model 425A DC Micro Volt-Ammeter was used to drive the Y channel of the Model 7000A recorder. The input impedance of the Model 425A ammeter varied from 0.010 MΩ up to 1 MΩ, depending on the range being used.

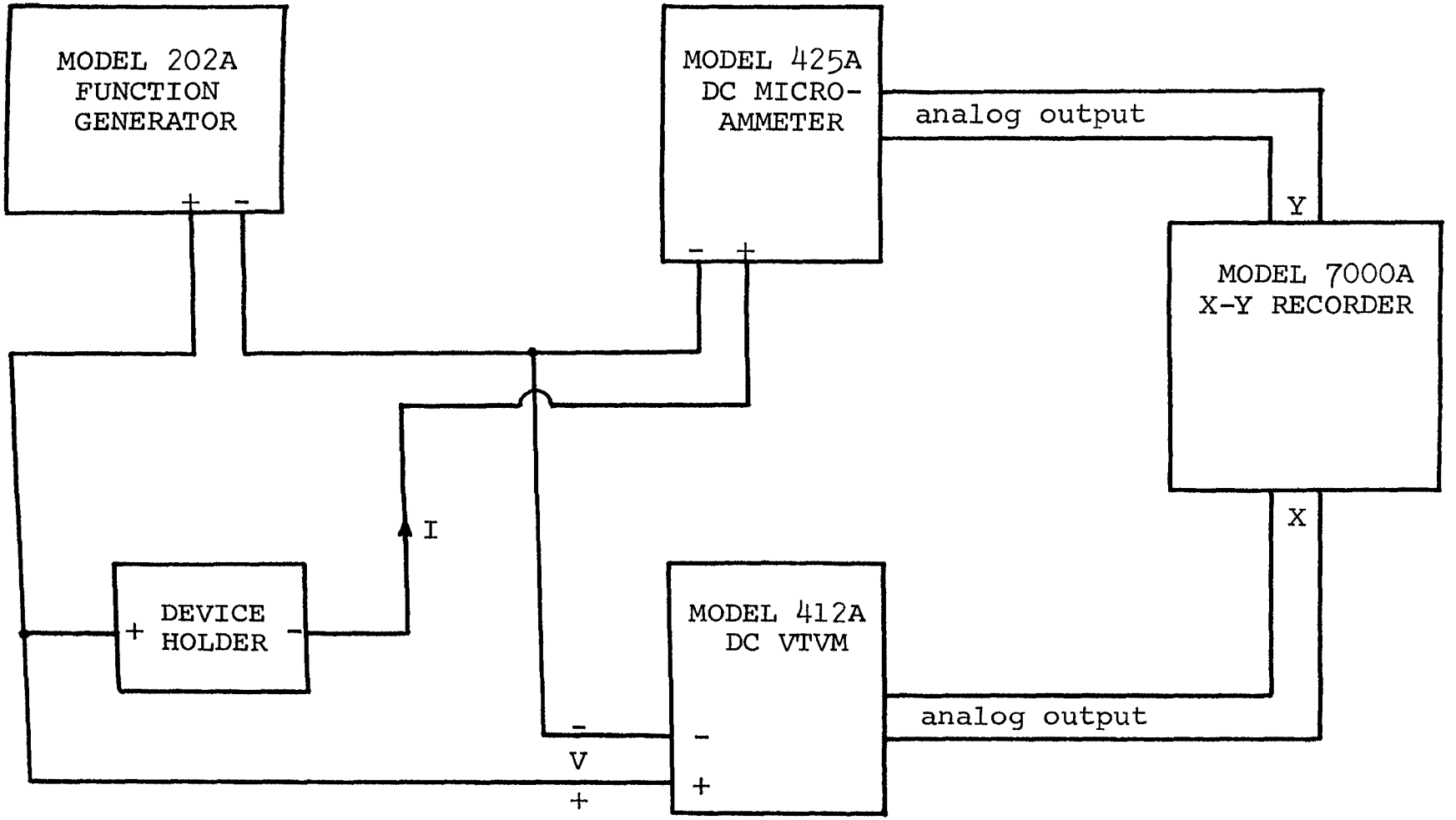


Figure 3. Block Diagram of Equipment Set-Up

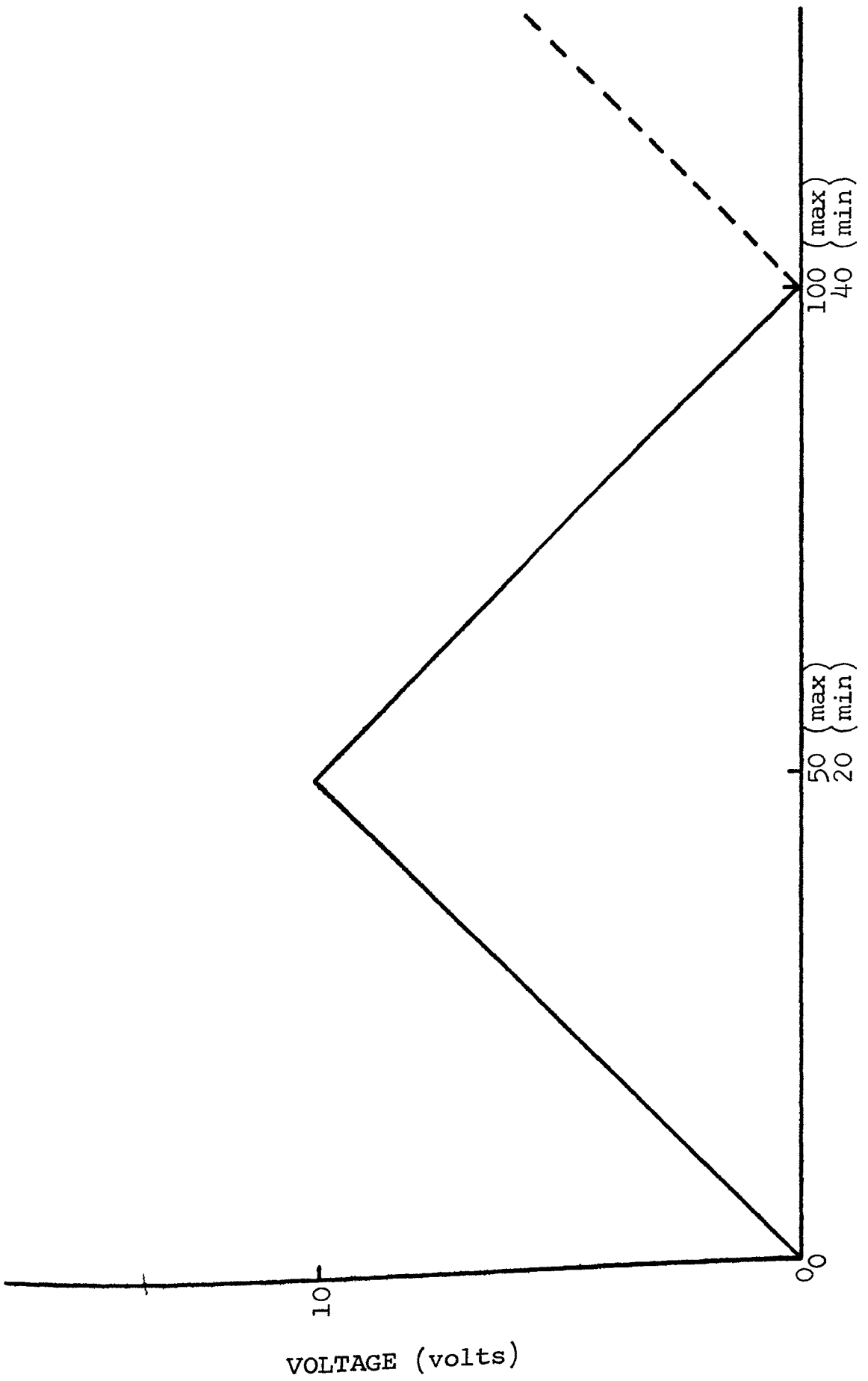


Figure 4. Output Waveform of Function Generator

# V. EXPERIMENTAL RESULTS

## A. General Results

A set of eight DC current-voltage characteristic curves were obtained for each of the devices listed in Table III. Each of the eight curves correspond to one of the eight possible device configurations which are listed in Table V. The devices were operated in the different configurations in order to determine if a certain configuration was necessary for them to exhibit the negative-resistance phenomenon.

The plots drawn in this document differ from those made by the X-Y recorder only in that they do not show the small amount of jitter which was introduced by the X-Y recorder.

The only device with which it was possible to obtain a reproducible negative-resistance phenomenon was device 16. That device only exhibited the phenomenon when it was operated in the A configuration, i.e., when half of the device, including the negative Ag contact, was masked to keep out visible light and the other half was exposed to visible light. Figure 5 is a plot of the DC current-voltage curves for device 16 operating in the A and the D configurations.

Device 12 also exhibited the phenomenon when operated in the A configuration, however the phenomenon was not reproducible and was observed only a few times. It was necessary to let device 12 rest in the dark for at least 24 hours between measurements in order to observe the phenomenon on a semi-reproducible basis.

TABLE V. Device Configurations

| CONFIGURATION TYPE | RECTIFYING CONTACT (Ag) POTENTIAL | DEVICE ILLUMINATION In CONTACT HALF | DEVICE ILLUMINATION Ag CONTACT HALF |
|---|---|---|---|
| A | Negative | Illuminated | Dark |
| B | Negative | Illuminated | Illuminated |
| C | Negative | Dark | Illuminated |
| D | Negative | Dark | Dark |
| E | Positive | Illuminated | Dark |
| F | Positive | Illuminated | Illuminated |
| G | Positive | Dark | Illuminated |
| H | Positive | Dark | Dark |

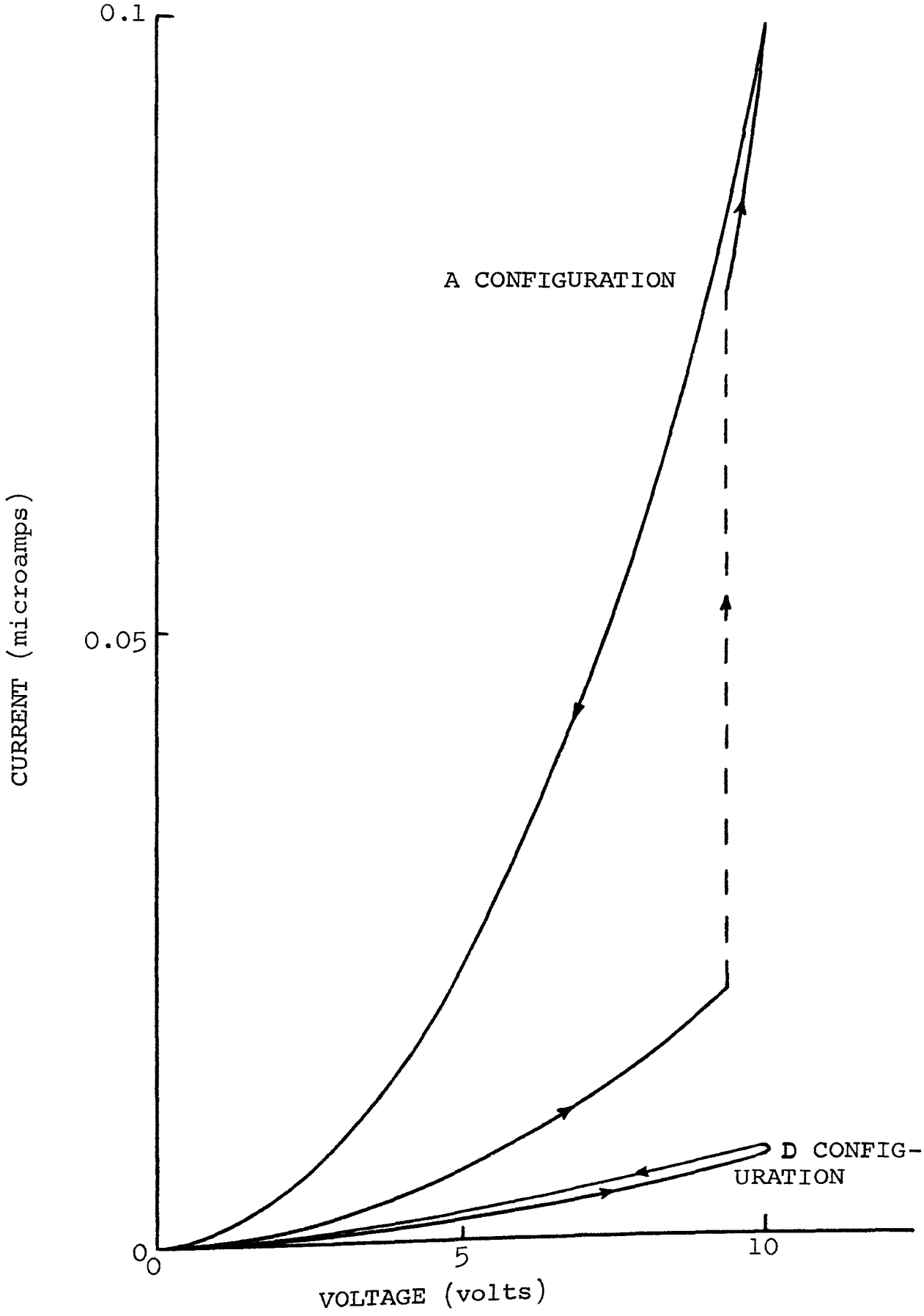


Figure 5. Current-Voltage Curves for Device 16 Operating in the A and D Configurations.

Device 12 and device 16 were both fabricated from the same CdS single crystal (number 1-S331). The longitudinal-axis orientation and the method by which the ohmic contact was applied were the only differences between device 12 and device 16. None of the other devices exhibited the negative-resistance phenomenon, not even on a nonreproducible basis.

In most cases, except those connected with the A configuration, the curves plotted for device 16 operating in the different configurations are typical of the curves obtained for the devices which did not exhibit the phenomenon.

B. Device 16 Results

Figure 6 is a plot of the DC current-voltage curve for device 16 operating in the A configuration. Portion BC of the curve shows the negative-resistance phenomenon. That portion of the curve is a switching from the lower curve portion AB to the upper curve portion ACD which is characteristic of the curve obtained by voltage sweeping a current-controlled negative-resistance device in the forward direction.

The shape of the negative-resistance portion of the curve could not be obtained for this device because of its high impedance (typically between 50 MΩ and 5000 MΩ). No attempt was made to measure the switching time for curve portion BC.

In order to obtain curve portion ABC, it was necessary to follow a series of steps which are: (1) allow the device to rest short-circuited in the dark for at least three

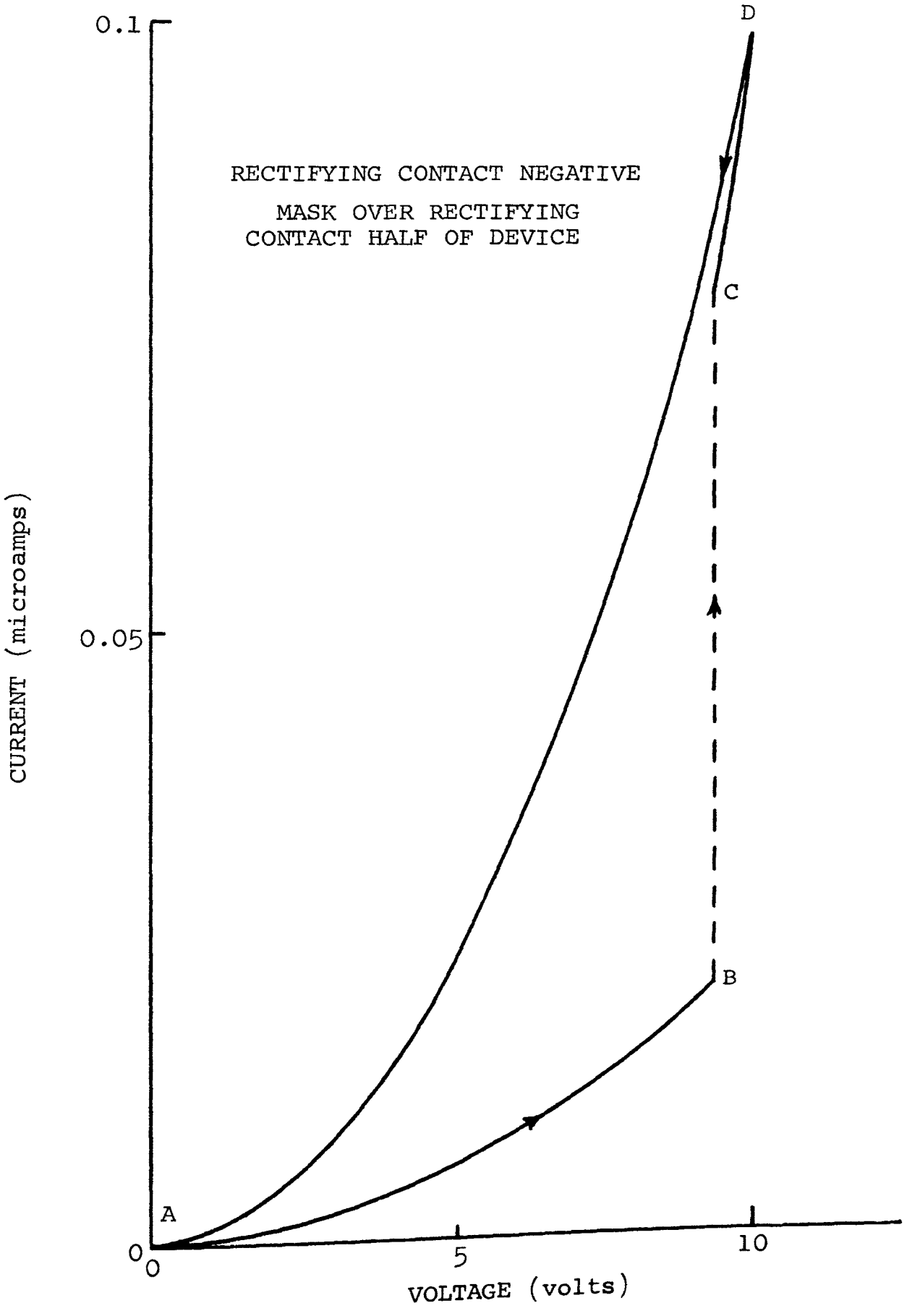


Figure 6. Current-Voltage Curve for Device 16 Operating in the A Configuration.

minutes between current-voltage measurements, (2) remove the short circuit, (3) open the device holder's cover and (4) start the voltage sweep at zero potential. It was found that the sweep period must be between 40 and 100 seconds. The optimum sweep period was approximately 70 seconds. If the steps were not followed, the device would operate on the upper curve portion ACD, i.e., give a curve similar to Figure 7 in appearance.

Figure 7 is a plot of the curve obtained by operating device 16 in the B configuration. The mask was removed for this measurement and the device was completely illuminated. The shape of this curve is typical of the shape of the curves obtained for the devices which did not switch, when they were operated in the A configuration. The hysteresis in this curve (and the other curves) is due to a difference in the excitation and decay times of the photo-current.

Figure 8 is a plot of the curve obtained by operating device 16 in the C configuration.

Figure 9 is a plot of the curve obtained by operating device 16 in the D configuration. This current-voltage measurement was made in complete darkness.

Figure 10 is a log-log plot of the same curve which is plotted in Figure 6, i.e., device 16 operating in the A configuration. The slope of the curves show that the current varies as the 2.2 power of the voltage for both the upper and lower portions of the curve.

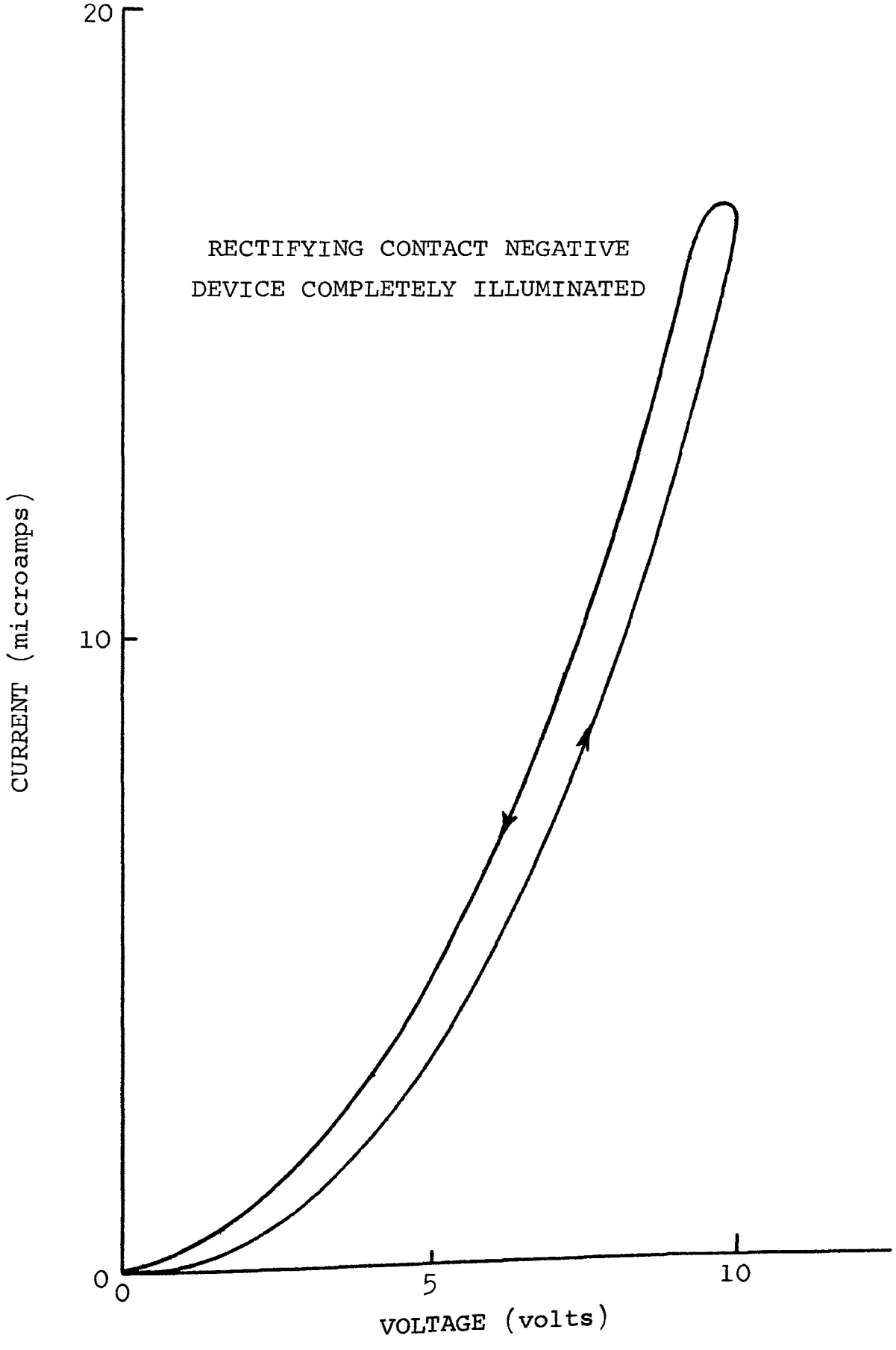


Figure 7. Current-Voltage Curve for Device 16 Operating in the B Configuration.

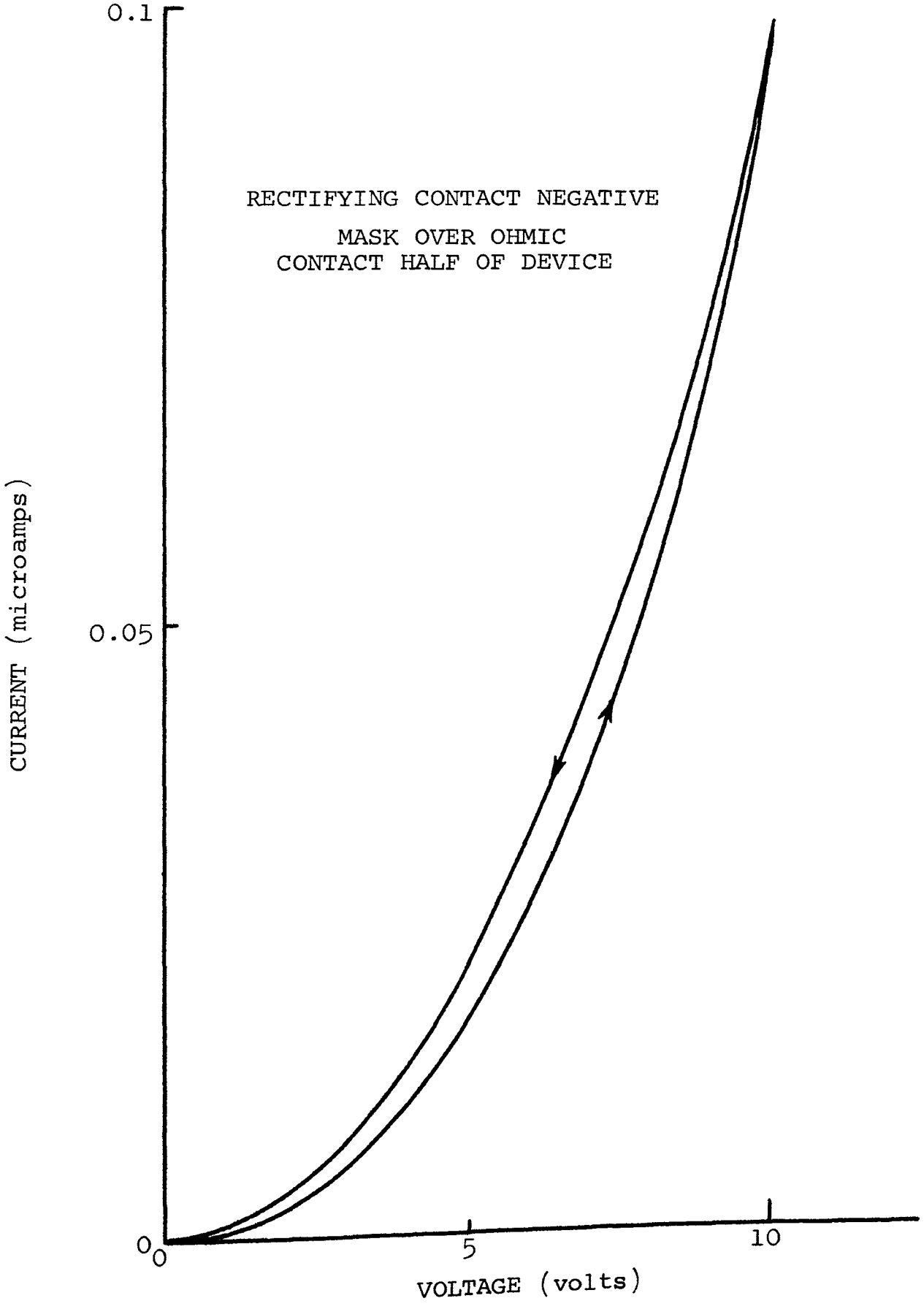


Figure 8. Current-Voltage Curve for Device 16 Operating in the C Configuration.

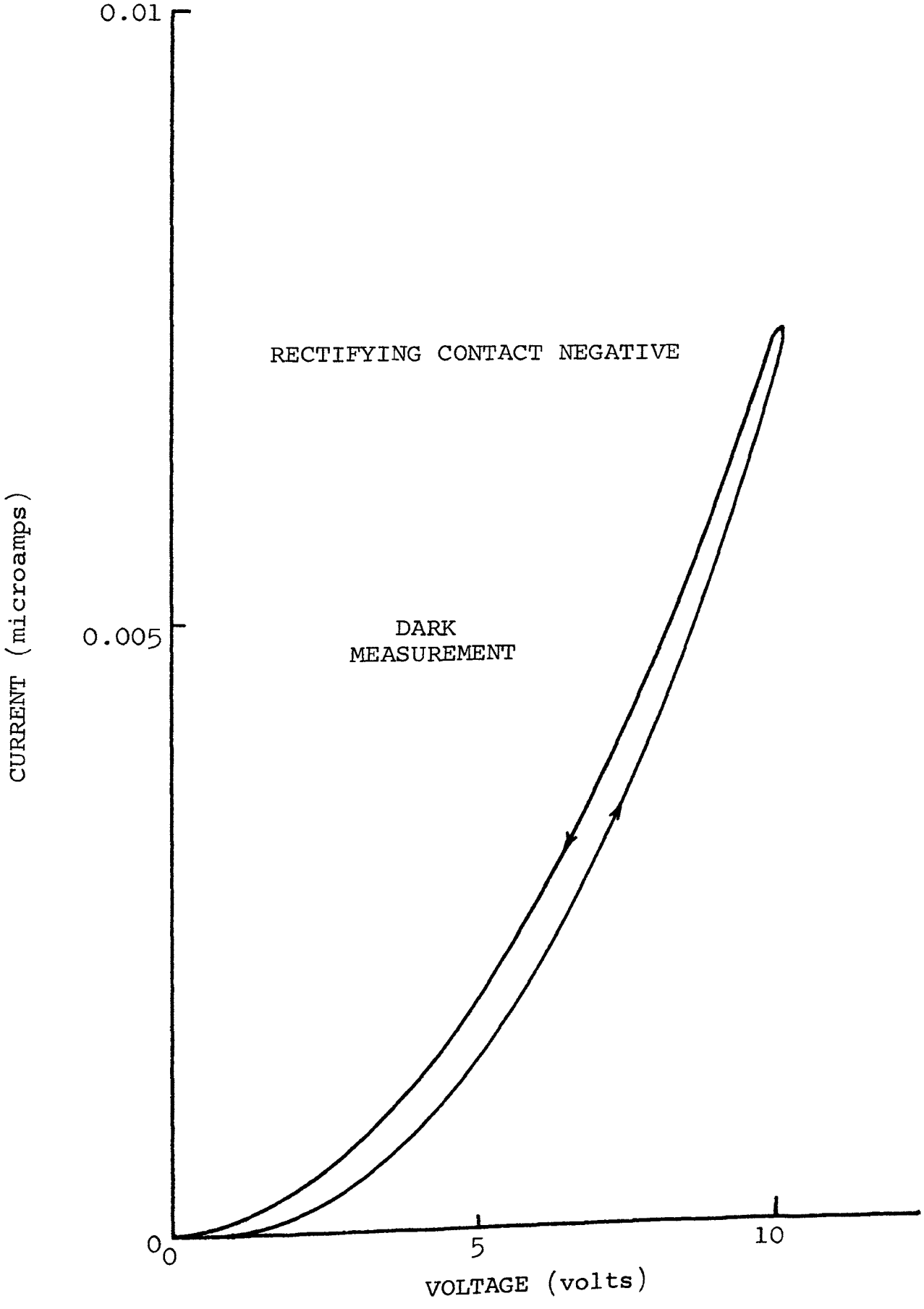


Figure 9. Current-Voltage Curve for Device 16 Operating in the D Configuration.

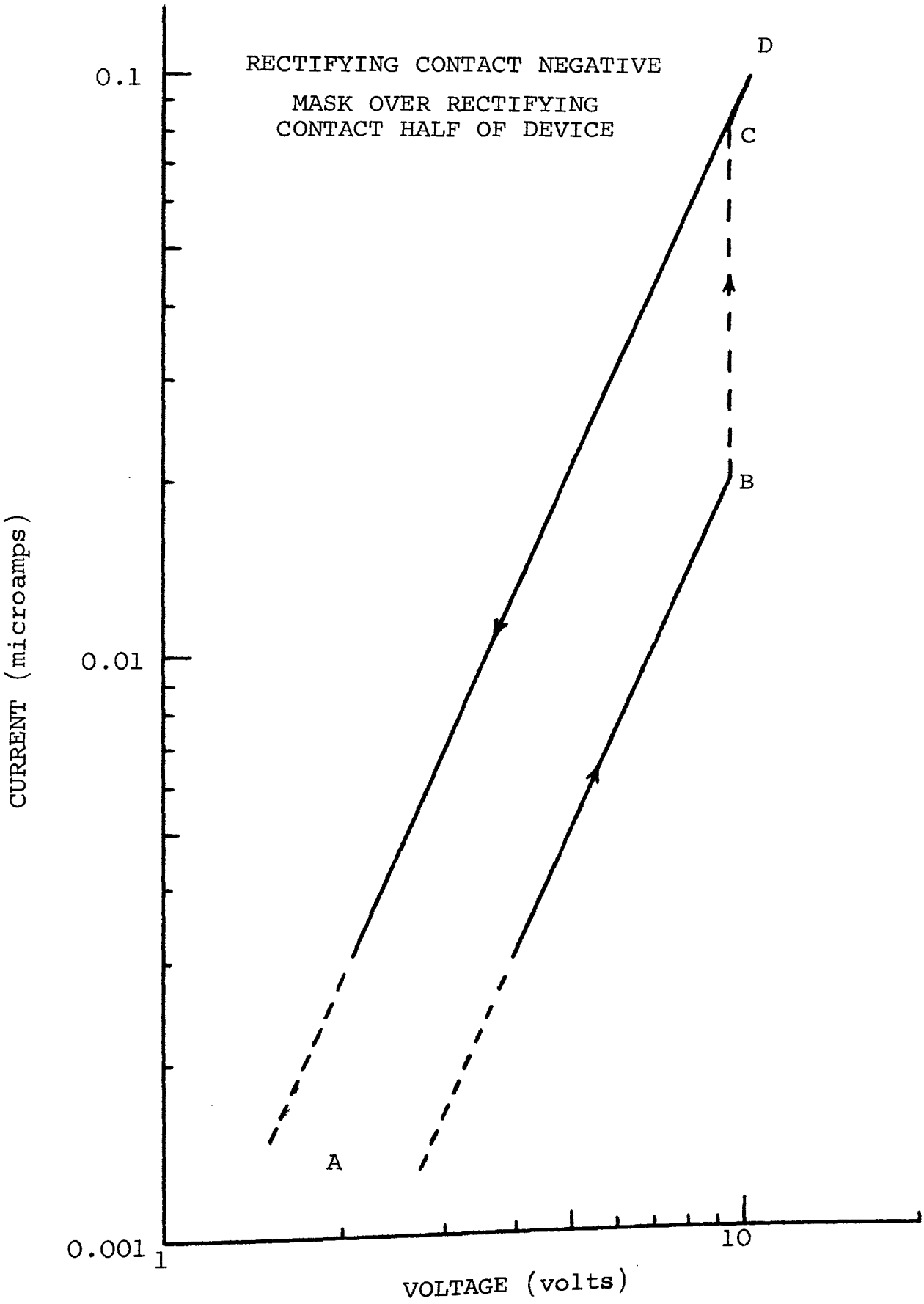


Figure 10. Log-Current Log-Voltage Curve for Device 16 Operating in the A Configuration.

Figure 11 is a plot of the curve obtained by operating device 16 in the E configuration. The E configuration is the same as the A configuration, with the exception that the device polarity is reversed.

Figure 12 is a plot of the curve obtained by operating device 16 in the F configuration. The mask is removed for this current-voltage measurement and the device was completely illuminated.

Figure 13 is a plot of the curve obtained by operating device 16 in the G configuration.

Figure 14 is a plot of the curve obtained by operating device 16 in the H configuration. This current-voltage measurement was made in complete darkness.

Figure 15 is a log-log plot of the same curve which is plotted in Figure 11. The slope of the curve shows that the current varies as the 4.34 power of the voltage.

Figure 16 is a plot of the curves obtained by operating device 16 in the A configuration at two different light intensities.

## C. Conclusions

Both devices 12 and 16, which did exhibit the phenomenon, were fabricated from the same CdS single crystal. This crystal had a relatively high density of traps (compared to the other crystals used in the investigation) and its properties are listed in Table VI.

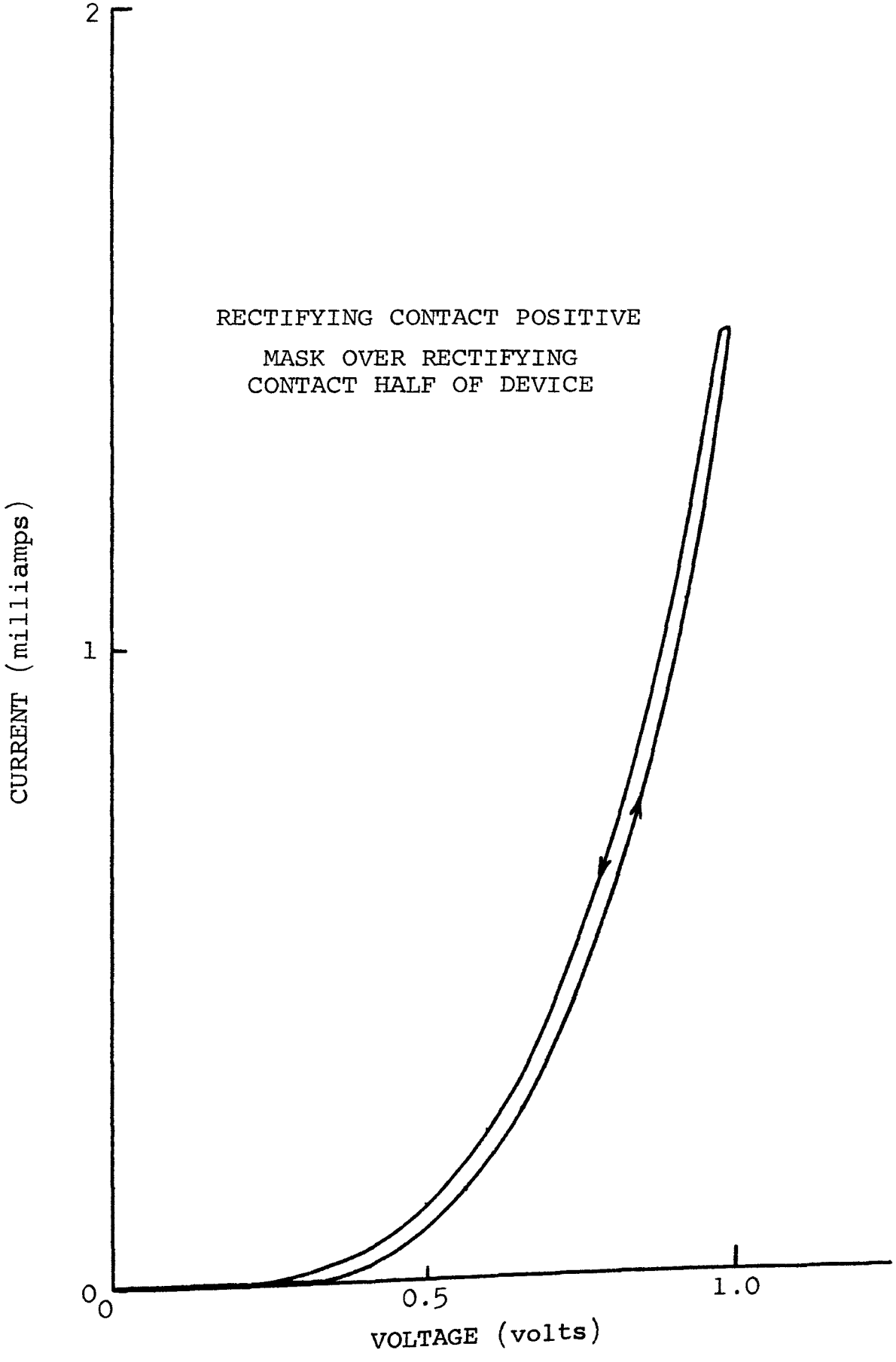


Figure 11. Current-Voltage Curve for Device 16 Operating in the E Configuration.

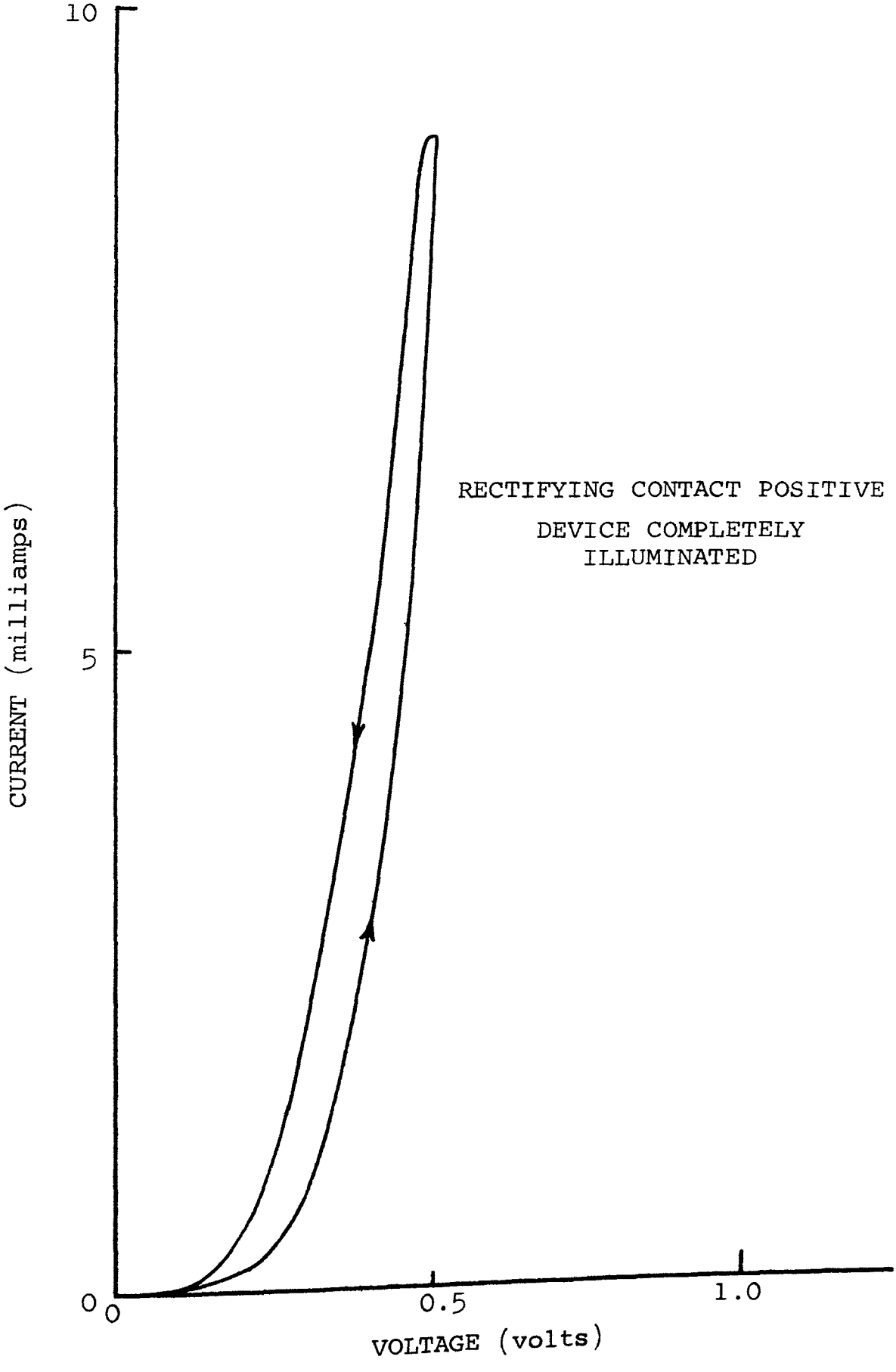


Figure 12. Current-Voltage Curve for Device 16 Operating in the F Configuration.

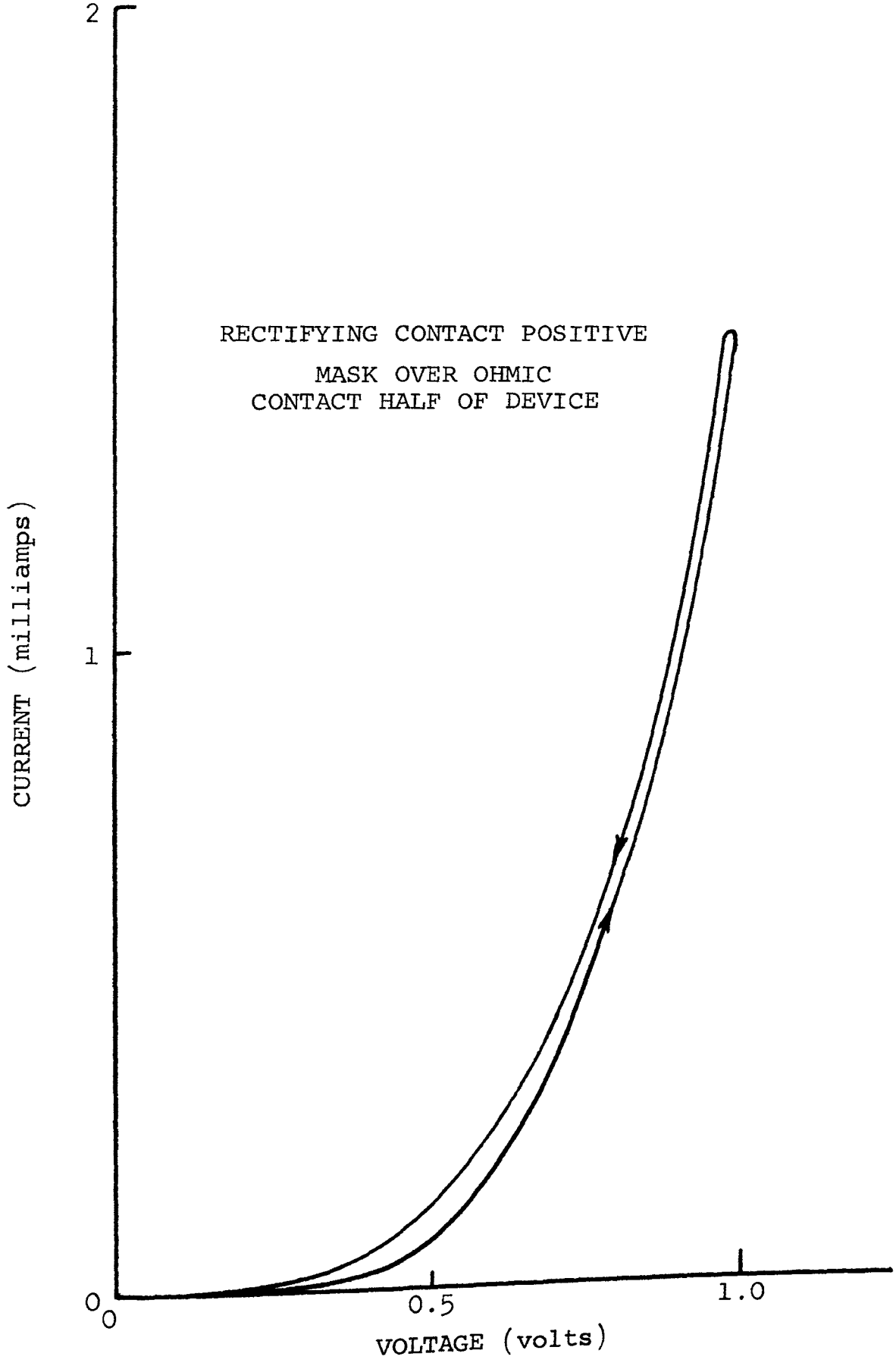


Figure 13. Current-Voltage Curve for Device 16 Operating in the G Configuration.

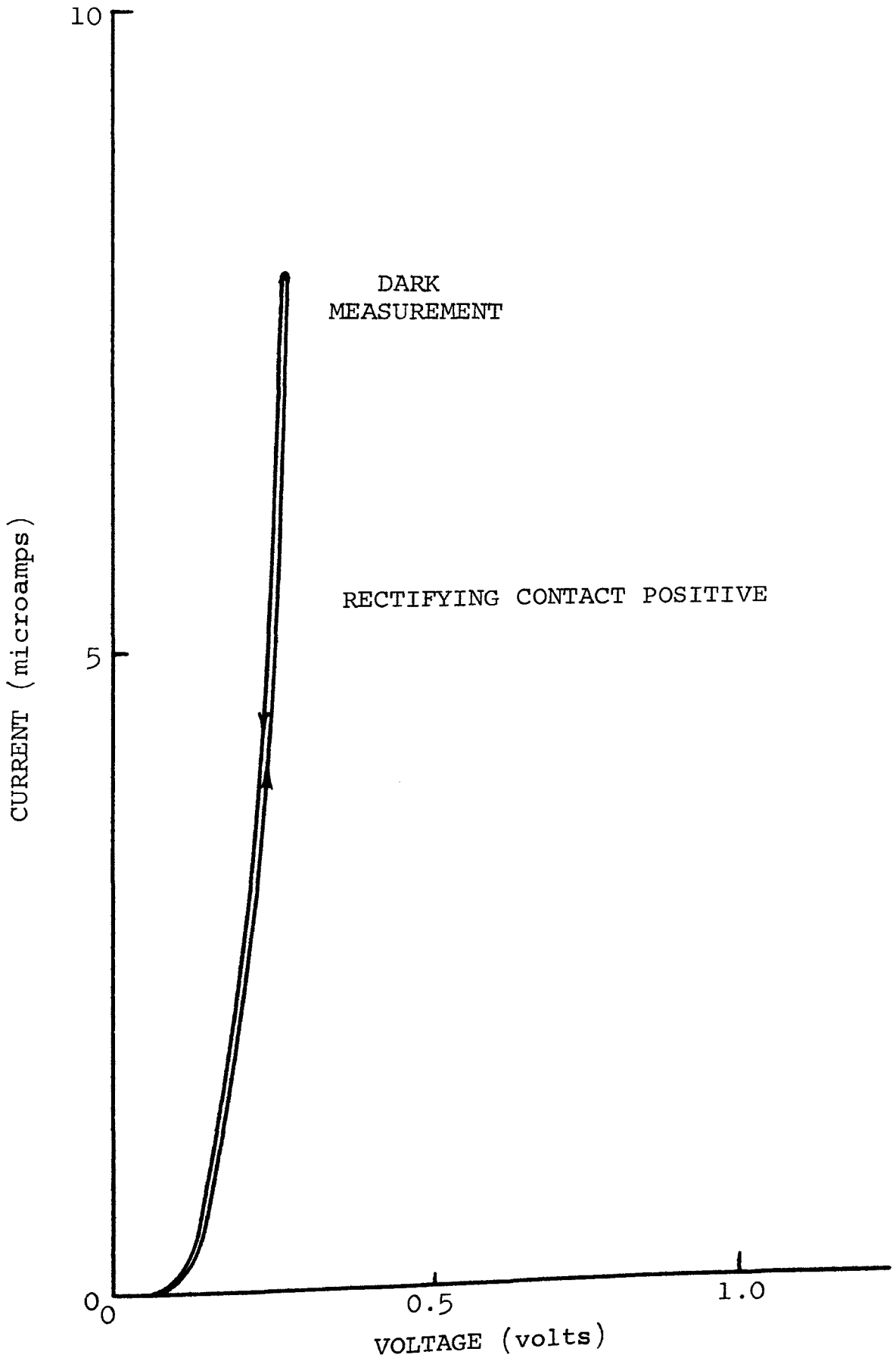


Figure 14. Current-Voltage Curve for Device 16 Operating in the H Configuration.

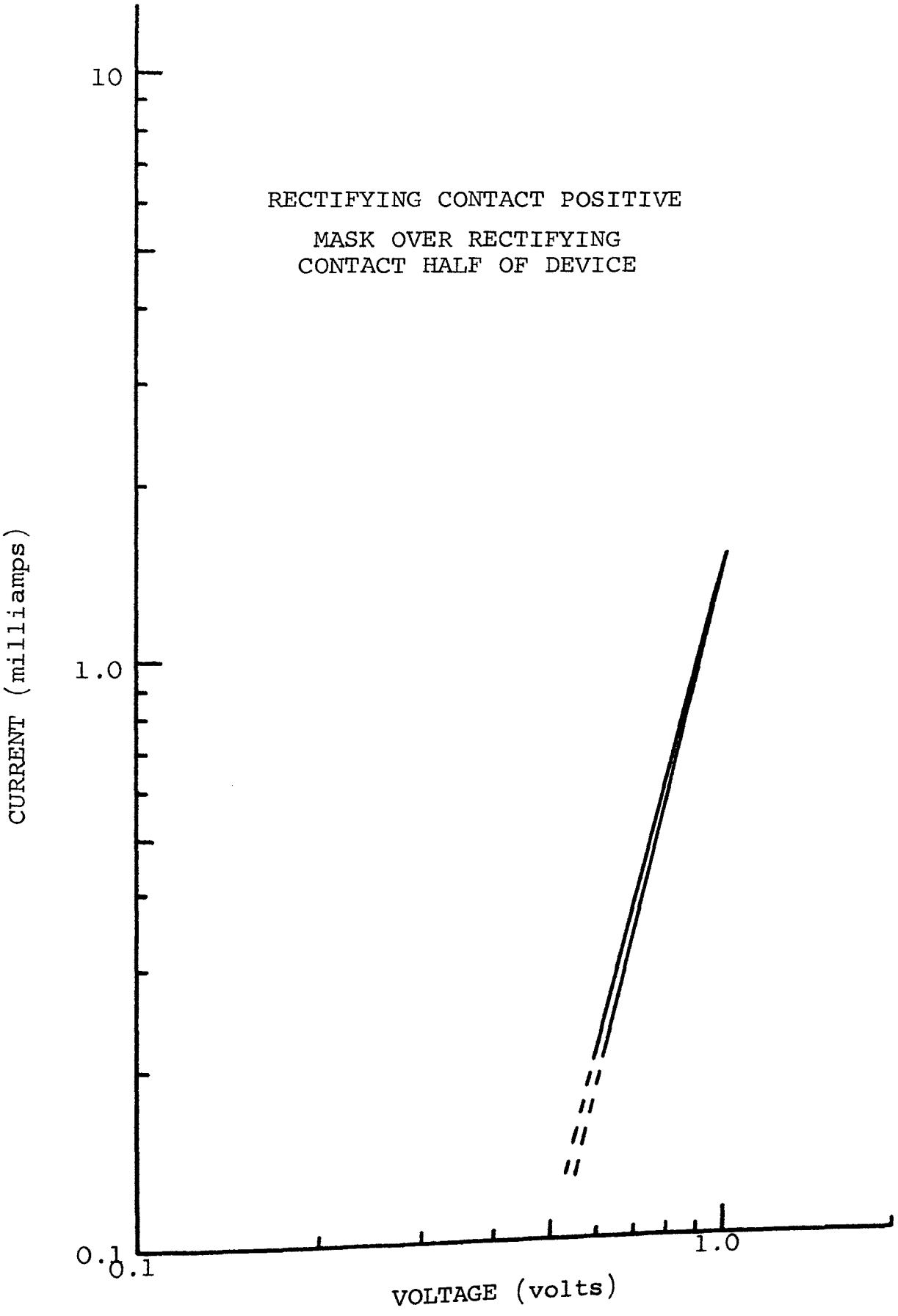


Figure 15. Log Current-Log Voltage Curve for Device 16 Operating in the E Configuration.

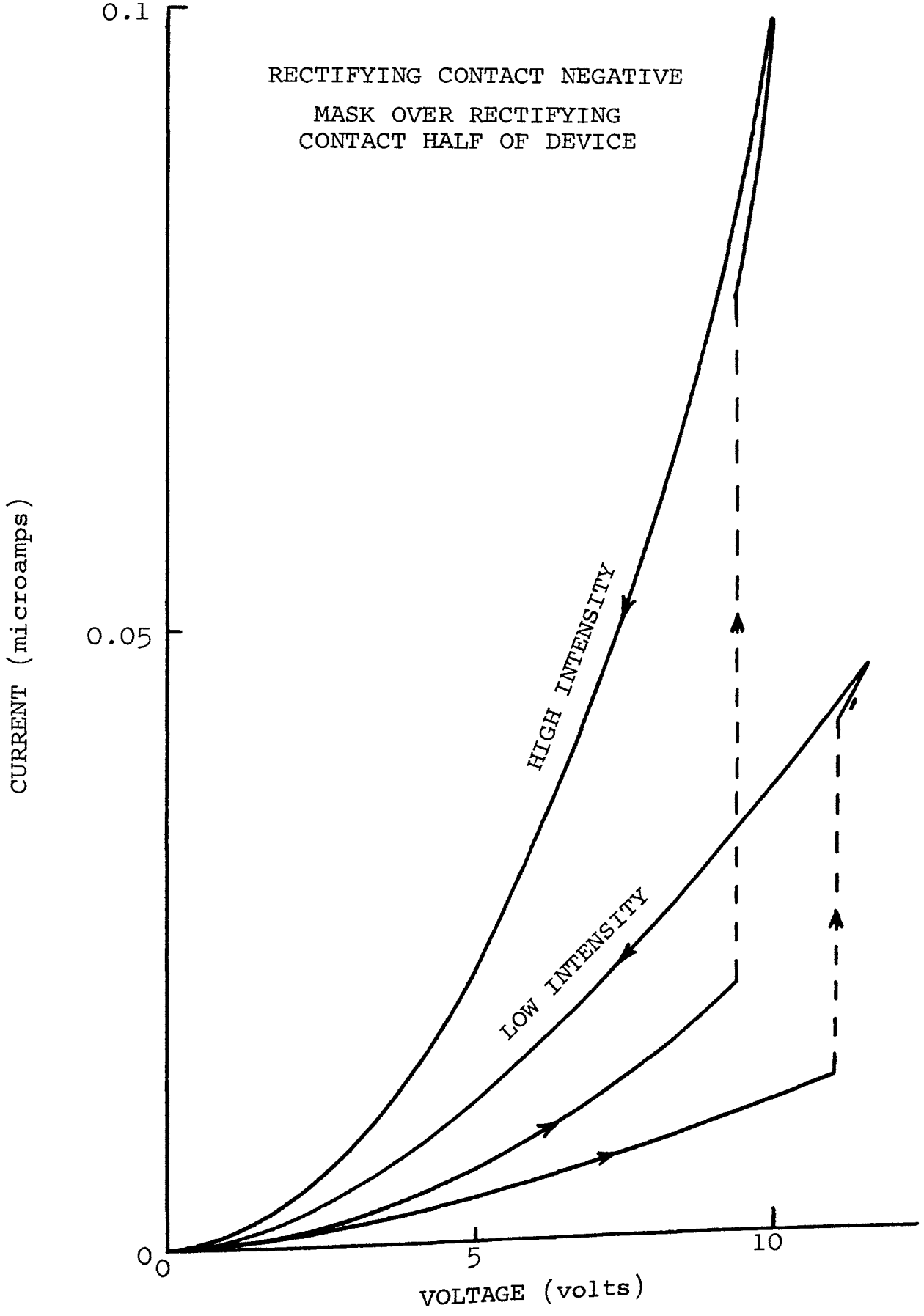


Figure 16. Current-Voltage Curves for Device 16 Operating in the A Configuration at Two Light Intensities.

Table VI. Properties of CdS Single Crystal 1-S331

SPECTROGRAPHIC ANALYSIS OF IMPURITIES (parts per million)

| | |
|---|---|
| Silicon | 2.0 |
| Copper | 1.2 |
| Indium (maximum) | 3.0 |
| Magnesium | 0.15 |
| Calcium | 0.03 |
| Zinc | 440.0 |

GRADE

Ultra High Purity

DOPING AGENT

None

RESISTIVITY

1 - 10 ohm-cm

As explained on page 39, traps play an important part in the phenomenon, which would account for the reason device 16 exhibited the phenomenon and other devices did not. Devices 17 and 18 were identical to device 16 with the exception that the single crystal (number 1-S331) became heated when the ohmic contact was applied. The heating annealed the single crystal, thus lowering the relative trap density which explains why device 16 exhibited the phenomenon and devices 17 and 18 did not. Device 12 was also annealed; however, it did exhibit the phenomenon on a nonreproducible basis. It seems that the trap density remained just large enough to allow the phenomenon to be observed only under ideal conditions.

Figure 10 and Figure 15, when compared, show that the device is not bilateral. This was to be expected because of the rectifying contact.

The combination of all the figures show that the device must be operated in the A configuration in order for it to exhibit the phenomenon. In other words, the correct polarity must be applied, the mask must be on the half of the device including the Ag contact, and the device must be illuminated.

# VI. POSSIBLE MECHANISMS

Determining the mechanism which causes the phenomenon will probably require further investigation of the device. Some possible mechanisms are described in this section.

The device is divided into an illuminated and a dark region. There is a high density of excess carriers in the illuminated region and a low density in the dark region if the applied voltage is small. The conductivity in the illuminated region is high because of the increased density of free carriers and also because the mobility is increased due to filled traps. By similar reasoning the conductivity in the dark region is very low. Excess carriers in the illuminated region tend to diffuse into the dark region but do not travel to the contact if the diffusion length is shorter than the length of the dark region. As an external voltage is applied, more carriers drift into the dark region. These additional carriers tend to fill the traps. The mobility then increases and eventually the diffusion length extends to the dark contact. The effect is similar to positive feedback in that: (1) an increase of carriers in the dark region causes (2) the mobility to increase by filling the traps which (3) makes it possible for more carriers to move faster and further in the dark region, and so on. This "regeneration" could give rise to the negative-resistance portion of the current-voltage characteristic when the region of higher carrier density extends to the masked contact.

Another explanation may be due to the fact that since trapping is present, both carriers are mobile but only one carrier is replenished at the ends of the device and a barrier is probably present at the rectifying contact. As an external voltage is applied to the device, the electric field across the contact barrier will change. The barrier may be broken locally, causing a sudden increase in the current due to the sudden participation of the other carrier in the current flow. This would explain the negative-resistance region if the voltage needed to sustain the barrier breakdown is less than that needed to cause the breakdown.

The electric field is probably a very complicated function of the distance along the device. This is further complicated by the fact that the electric field distribution is constantly changing as the applied voltage is changed. Measurements to determine the electric field strength along the length of the device as a function of time, might be helpful in determining the mechanism. Such time varying measurements would be difficult to obtain because of the high resistance of the device.

# VII. SUMMARY AND RECOMMENDATIONS

## A. Summary

The most important findings to come out of the investigation can be summarized as follows: (1) the negative-resistance phenomenon was observed and a method was found to make the phenomenon reproducible, (2) it was found that the CdS single crystal must have a relatively high density of traps and therefore annealing the crystal should be avoided, (3) the device is not bilateral, (4) the device does not exhibit the phenomenon in the dark, (5) the device must be operated in one certain configuration in order for it to exhibit the phenomenon and (6) the period of the sweep voltage waveform must be kept between certain limits.

## B. Recommendations for Further Studies

The investigation described in this document can be extended in many different ways.

The most important extension would be the actual determination of the mechanism which causes the phenomenon. This would probably be a difficult problem and require many different measurements to be made on the CdS single crystal as well as the device itself. Parameters such as trap depth, mobilities, diffusion constants and diffusion lengths may be needed.

A study of the effects of different illumination frequencies, illumination intensities, ambient temperatures

and crystal orientation may point toward some optimum operating conditions and a better understanding of the mechanism.

An investigation could be performed to determine the optimum geometry so that the switching time could be minimized. The geometrical size of the device and the relative positions of the contacts could be optimized experimentally.

The fact that the period of the sweep voltage waveform must be kept within certain limits indicates that certain lifetimes are a determining factor in the observation of the phenomenon. An investigation to relate the sweep voltage period to the lifetimes could be useful in understanding the phenomenon.

# BIBLIOGRAPHY


1. Dillman, N. G., (1964) Autonetics Patent File Number 64EG31.

2. Lampert, M. A., (1962) Double Injection in Insulators. Phys. Rev. 125, p. 126-141.

3. Smith, R. W., (1957) Low-Field Electroluminescence in Insulating Crystals of Cadmium Sulfide. Phys. Rev. 105, p. 900-904.

4. Litton, C. W., and D. C. Reynolds, (1964) Double-Carrier Injection and Negative Resistance in CdS. Phys. Rev. 133, p. A536-A541.

5. Hansch, H. J., E. Nebauer and M. Nikolaus, (1965) Experimental Investigations of Thermally Induced Negative Differential Resistances. Phys. Status Solidi. (Germany) 12, p. 93-100.

6. Takagi, T., and Y. Mizushima, (1967) Properties of Breakdown and Switching in CdS Single Crystals. Proc. IEEE 55, p. 477-478.

7. Ridley, B. K., (1963) Specific Negative Resistance in Solids. Proc. Phys. Soc. (London) 82, p. 954-966.

8. Guerce, J. C., B. Melchiorri and F. Melchiorri, (1965) Spontaneous Photocurrent Oscillation in CdS Generated by a Tranverse Electric Field. Phys. Letters (Netherlands) 18, p. 243-244.

9. McLeod, B. R. and R. E. Hayes, (1965) Current Oscillations in Cadmium Sulfide. Proc. IEEE 53, p. 1772-1773.

10. Yee, S., (1965) Experimental Evidence of High Field Domain in Dark Conductive CdS. Proc. IEEE 53, p. 1763-1764.

11. Harnik, E., (1965) Quenching and Enhancement of the Dark Conductivity in High-Resistivity, Photosensitive Single Crystals of Cadmium Sulfide. Solid-State Electronics (GB) 8, p. 931-937.

12. Smith, R. W., (1951) Some Aspects of the Photoconductivity of Cadmium Sulfide. RCA Rev. 12. p. 350-361.

13. Bube, R. H., (1960) Photoconductivity of Solids. New York, Wiley, p. 83-87.

14. Stockman, F., (1965) Photoconductivity Conference. New York, Wiley, p. 269-286.

15. Rose, A., (1951) An Outline of Some Photoconductive Processes. RCA Rev. 12, p. 362-414.

16. Van Heerden, P. J., (1957) Primary Photocurrent in Cadmium Sulfide. Phys. Rev. 106, p. 468-473.

# VITA

John William Mohr was born on August 27, 1943, in St. Louis, Missouri. He received his primary and secondary education in St. Louis. He entered The Missouri School of Mines and Metallurgy in September, 1961, and received a Bachelor of Science Degree in Electrical Engineering in January, 1966.

He has been enrolled in the Graduate School of The University of Missouri at Rolla since January, 1966, and was appointed as a Graduate Assistant for the period January, 1966, to June, 1966, and as a Research Assistant for the period September, 1966, to August, 1967.